Available online at www.sciencedirect.com
ScienceDirect
Physics of the Earth and Planetary Interiors xxx (2007) xxx–xxx
PHYSICS OF THE EARTH AND PLANETARY INTERIORS
www.elsevier.com/locate/pepi

Tsunami hazards along Chinese coast from potential earthquakes in South China Sea

Yingchun Liu [a,b,*], Angela Santos [d], Shuo M. Wang [c], Yaolin Shi [b], Hailing Liu [a], David A. Yuen [c]

[a] South China Sea Institute of Oceanology, Chinese Academy of Sciences, Guangzhou, China
[b] Graduate University of Chinese Academy of Sciences, Beijing, China
[c] Department of Geology & Geophysics and Minnesota Supercomputing Institute, University of Minnesota at Twin Cities, Minneapolis, MN, USA
[d] Tsunami Engineering Laboratory Disaster Control Research Center School of Engineering, Tohoku University, Japan

Received 19 January 2007; accepted 23 February 2007

Abstract

The pair of earthquakes off Taiwan on December 26, 2006 and the subsequent disruption of the Internet traffic have called attention to the potential destructive hazards along the Chinese coast from tsunamis. Historical records show past tsunami earthquakes in this region. Using GPS, earthquake focal mechanisms and geological evolution, we have delineated the dangerous zones in the Philippine Sea plate where major earthquakes may occur. The Manila Trench is identified as being most susceptible to future major earthquakes. We have obtained the local Gutenberg–Richter relationship for five sections along the Philippine Sea plate boundary and use this information for determining the probability distribution for tsunami waves of various heights to impinge on various Chinese cities. We devise a new method called the probabilistic forecast of tsunami hazard (PFTH), which determines this probability distribution by direct numerical simulation of the waves excited by hypothetical earthquakes in these zones. We have employed the linear shallow-water equations over the South China Sea. We have also compared them with results from the nonlinear version and found that the linear treatment serves our purpose sufficiently well. In the next century the probability of a wave with a height of over 2.0 m to hit Hong Kong and Macau is about 10%. Cities in Taiwan are less vulnerable than those on the mainland coast.

PACS: 07.05.Rm; 91.30.P; 91.30.Nw; *92.10.hl; *91.30.P; 91.30.Px; 91.30.Zz

Keywords: Tsunami hazard; Numerical simulation; Earthquake probability; Shallow-water equation; South China Sea

1. Introduction

Tsunamis occur around the world from various causes, principally from shallow earthquakes in subduction zones. Around 90% of the global undersea earthquakes take place around the circum-Pacific belt. Once again on December 26, 2006 we were alerted to the danger of tsunami hazards along the East China coast

* Corresponding author at: Digital Technology Center, Room 413, Walter Library, 117 Pleasant St. SE, Minneapolis, MN 55455, USA. Tel.: +1 612 624 6730.
E-mail addresses: liuyingch@mails.gucas.ac.cn, spring.yingch@gmail.com (Y. Liu), angela@tsunami2.civil.tohoku.ac.jp (A. Santos), shwang1386@gmail.com (S.M. Wang), shiyl@gucas.ac.cn (Y. Shi), liuh8@scsio.ac.cn (H. Liu), daveyuen@gmail.com (D.A. Yuen).

0031-9201/$ – see front matter © 2007 Published by Elsevier B.V.
doi:10.1016/j.pepi.2007.02.012

by the Pingtung earthquakes off southern Taiwan. This area is prone to large subduction related tsunamogenic earthquakes because of the nature of the complex plate boundary, ranging from Taiwan in the north to the Manila Trench in the south. Until the end of 2004, there was little awareness about the potential tsunami danger from shallow large earthquakes in this region with great economic importance. We must now be prepared to set up a suitable system for broadcasting tsunami warnings in the South China Sea area.

Tsunami earthquakes take place most likely in trench regions with a large tectonic movement and young folded crustal belts. The South China Sea with the adjacent Philippine Sea plate bordered by the Manila Trench is an excellent candidate for such devastating waves to occur. Moreover, the coastal heights along the South China Sea are generally low, thus making it extremely vulnerable to incoming tsunami waves with a height of only a couple meters. In particular, many economically important coastal cities, such as Hong Kong and Macau, are only a couple of meters above the sea level, and would suffer a large-scale disaster, even if the height of the tsunami wave were moderate.

Scientists have provided long records of past tsunamis, going back for the past two thousand years along the Chinese coast (Table 1) that clearly portends the potential danger of impending tsunami damages. The most devastating tsunami in this region occurred 140 years ago (in 1867) in Keelung at the northern tip of Taiwan. Both the northeast and southwest coasts of the Taiwan Island have higher possibility from impending tsunamis because of their closeness to plate boundaries.

In this work we will employ PFTH to analyze the probability for tsunami waves of various heights to hit the cities along the Chinese coast in this century. These waves are assumed to be caused by large earthquakes originating from the dangerous Manila Trench. This analysis becomes evermore crucial because of the sharp increase in the coastal population density in China, and the intensive growth of harbors and the exploration of mineral resources in the coastal areas, ranging from Xiamen in the north to Hainan in the south. In this paper we report our results on tsunami hazards prediction along the South China Sea bordering regions from potential earthquakes coming from the Manila Trench. We hope this paper will spur greater interest from countries around the Pacific Ocean in fundamental research in earthquakes, tectonics and geodetics in this area.

2. Geological and geophysical analysis

The South China Sea (Fig. 1), which lies on the western part of the Pacific Ocean, is one of the largest marginal sea along the continental margin of East Asia, covering an area around 3,500,000 km^2, almost as large as three times that of the Bohai Sea, Yellow Sea and East China Sea combined together. The South China Sea, along with Taiwan and the Philippines island arc-trench to its east, constitute a very complex channel-basin structural system. Bordered by the Eurasia continent, Pacific and Indian Ocean, the South China Sea belongs to the transitional crust between the oceanic and continental crust tectonic zone. Complex geological structures are reflected in the large-scale mass movement along the horizontal directions in this region, which is often accompanied with extensive vertical movement. The South China Sea spreads from the center and subducts along the Manila Trench (Liu et al., 1988).

The crust of this region is under tremendous tectonic stresses from many directions due to the complex interactions among three plates mentioned earlier. As illustrated in Fig. 1, a few deep faults surrounding the South China

Table 1
Historical records of the tsunamis along China coast (Wang and Zhang, 2005)

Wave incidence	Time	Epicenter	Magnitude
Gulf of Penglai, Bohai	April 4, 171		
Gulf of Laizhou, Bohai	July, 173		
Jiangsu and Zhejiang	July 9, 1496	South Sea of Japan	≥8
Quanzhou, Fujian	December 29, 1604	(24.7°N, 119.0°E)	7
Qiantangjiang, Zhejiang	October 28, 1707	(33.2°N, 135.9°E)	8.4
Tainan, Taiwan	August 9, 1792	(23.6°N, 120.6°E)	7
Keelong, Taiwan	December 18, 1867	(25.25°N, 122.2°E)	[a]
Keelong, Taiwan	July 4, 1917	(25.0°N, 123.0°E)	7.3[b]
Huangzhou, Fujian	February 13, 1918	(23.6°N, 117.3°E)	7.3
Yantan, Shandong	July 13, 1923	(31.0°N, 130.5°E)	7.2
Huanlien, Ilan, Taiwan	November 15, 1986	(24.1°N, 121.7°E)	7.6

[a] Wave height 7.5 m.
[b] Wave height 3.7 m.

Please cite this article in press as: Liu, Y. et al., Tsunami hazards along Chinese coast from potential earthquakes in South China Sea, Phys. Earth Planet. Interiors (2007), doi:10.1016/j.pepi.2007.02.012

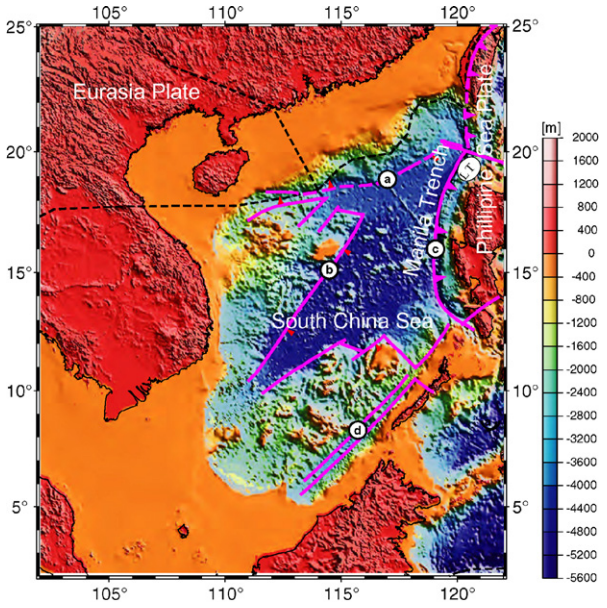

Fig. 1. Major deep faults of the South China Sea and its adjacent regions. (a) North margin fault of the Central Basin of SCS. (b) Western margin fault of the Central Basin of SCS. (c) Manila Trench. (d) Nansha trough fault. Figure is adapted from Liu et al. (1988). LT, Luzon trough. Green stars represent the historical seismic tsunamis catalog from NGDC/NOAA. (For interpretation of the references to color in this figure legend, the reader is referred to the web version of the article.)

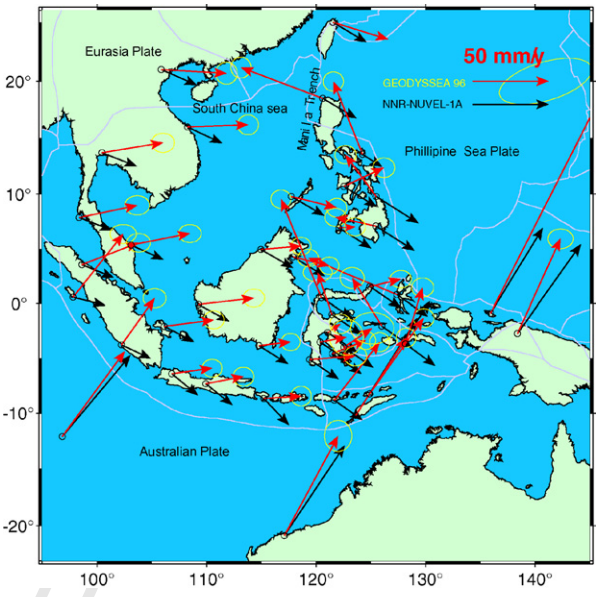

Fig. 2. Site motions in ITRF96 reference frame derived using GPS observation campaigns in 1996 (GEODYSSEA) together with those extracted with NNR-NU-VEL-1A model.

Sea, including the northern margin of the Central Basin, the western edge fault, the Manila Trench, and the Nansha Trough fault (Liu et al., 1988), dominate the crustal structure and depth distribution.

All these faults divide the region with two different types of crusts, continental and oceanic. At the inner side of these faults is the Central Basin of the South China Sea, which belongs to oceanic tectonic plate. The northern margin fault (Fig. 1(a)) of the South China Sea extends along Northern-East East (NEE) direction. It consists by the northern continental and the southern transitional crust. The western edge fault of the South China Sea is located at the east of Pratas Islands (Fig. 1(b)). To the west of the fault is Zhongsha, Xisha island slope, which belongs to a transitional crust. This fault belongs to a class of normal expansion faults. The Manila Trench (Fig. 1(c)) is located at the east boundary of the Central Basin of South China Sea, in the direction of South–North (SN). The fault is formed by the compressive fault structure with reverse fault motion. To the Northeast of the trench is a transitional crust of Luzon trough. Along the NE direction, the Nansha trough fault (Fig. 1(d)) is formed by the compressive fault structure. Its northern part has a tensile edge, while the western part has a shear edge and the eastern part and southern part are boundaries being compressed.

Based on the history of geological evolution and the present tectonics of the South China Sea, the Manila Trench and the north fault system have been in compression for long time with the Eurasian plate and Philippines plate.

In order to comprehend the modern stress field of the South China Sea, we have pooled various data resources together by including the seismotectonic information from the literature, seismic records (Harvard CMT solutions), information from global plate reconstruction models (NUVEL-1A) and geodetic data (Fig. 2). The geodetic data come from the GEODYSSEA (Geodynamics of South and South-East Asia) project, which has the working title of the project "Plate motions and crust deformations deduced from space geodetic measurements for the assessment of related natural hazards in South-East Asia," with the aim of studying the plate motions and long-term crustal deformation in Southeast Asia using a GPS network covering area of 4000 km × 4000 km (Wilson et al., 1998). In the GEODYSSEA campaign the inferred motion of the Sundaland block (Simons et al., 1999), it was characterized by using site motions on the stable core of this block (Becker et al., 2000). We note that the Manila Trench is predicted in a convergent direction by the relative NUVEL-1A model and/or GEODYSSEA measurements motions of the adjoining blocks. According

Please cite this article in press as: Liu, Y. et al., Tsunami hazards along Chinese coast from potential earthquakes in South China Sea, Phys. Earth Planet. Interiors (2007), doi:10.1016/j.pepi.2007.02.012

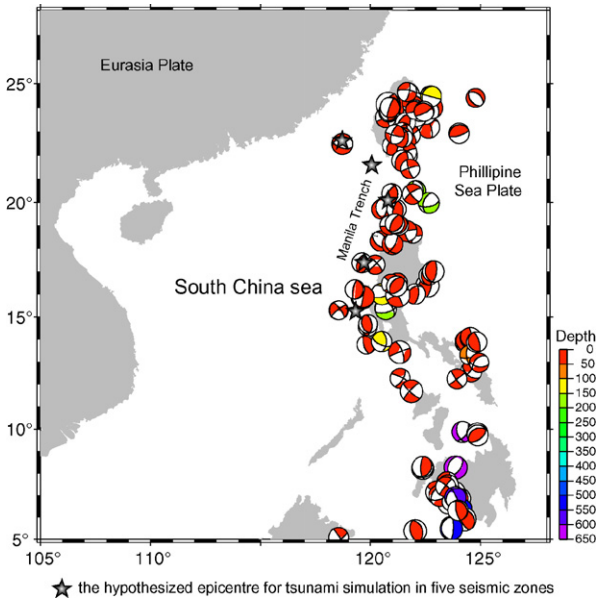

Fig. 3. The distribution of seismic focal mechanism of the South China Sea and its adjacent regions. The magnitude is ≥6.0. Data derived from Harvard CMT solutions (1976–2006).

to GEODYSSEA data, the Eurasia plate moves toward the northwest at nearly 10 mm/year in this region. While the Philippine Sea plate moves from east to west at a speed of 50 mm/year. These activities indicate that this is a region with highly active plate motion. As suggested by Michel et al. (2001), the greatest accumulated deformations have been accommodated by seismic faulting along the Manila Trench according to the geodetic study by assuming that the geodetic deformation represents the tectonic loading in the brittle part of the crust.

The analysis of the focal mechanism solutions (Fig. 3) (Harvard CMT solutions) reveals that the stress states of the Manila Trench and its adjacent region are different. In the northern part of the Manila Trench, and the adjacent Philippine faults, the focal mechanism solutions show the evidence of the compressive-thrusting. On the other hand, in the southern region of the Manila Trench, the stress distribution becomes very complex. Along the two sides of western Luzon trough close to the trench, the focal mechanism solutions show an oblique-strike with normal faulting, and in front of the diving zone away from the trench they show a thrusting character. Local seismic focal mechanism solutions also indicate high cumulative moment rates from data taken over last 30 years in the Manila subduction segments.

According to Zang and Ning (2002)'s research, the eastern boundary of Philippine Sea plate is a convergence zone dominated by subduction, where the earthquakes are concentrated. The principal stress field tensor of this region is nearly along the North-West West (NWW) direction. Subduction of the oceanic crust of the Central Basin of South China Sea is reduced in the Taiwan–Philippine island arc region. The majority of the earthquakes are distributed around South Taiwan and the Philippines, especially along Manila Trench fault and Luzon trough, which is arranged into striped patterns.

However, the present-day earthquakes are not distributed evenly along the plate boundaries and historical seismic records indicate that the Manila Trench has been highly affected by major earthquakes in the north-western part of Philippines (shown in Fig. 5(a)). Furthermore, major earthquakes along the Manila Trench with a higher frequency have also influenced the stress state of southern Taiwan. Thus the geological evolution, the GPS velocity field, CMT background and seismic distribution provide sufficient evidence that is a focussing of the potential seismic energy along the Manila Trench.

3. Probabilistic forecast of tsunami and seismic hazards

We devise a method called Probabilistic Forecast of Tsunami Hazard (PFTH), which determines this probability distribution by direct numerical simulation of the waves excited by the earthquakes. Our probabilistic forecast of tsunami hazard (PFTH) consists of the following three steps:

(1) *Probabilistic Forecast of Seismic Hazard* (*PFSH*). The probability and locations of earthquakes are estimated.
(2) *Tsunami modeling*. For each earthquake predicted, its hydrodynamical influence of the waves reaching each coast location is computed based on the results of our tsunami wave height simulation with the Shallow-water equation.
(3) *Probabilistic forecast of tsunami hazard* (*PFTH*). The sum of tsunami risks of all possible large earthquakes provides the statistical risk distribution.

In contrast to the work of Geist and Parsons (2006), which estimated tsunami probability only from earthquake magnitudes, we have determined the tsunami probability by using the wave height at each station by numerically solving the shallow-water equations. Our method, based on simulations, is different from empirical methods (Geist and Parsons, 2006) and is valuable in areas where these are not to many historical records.

In our method, PFSH is conducted by using several sources. First, the major earthquake occurrence proba-

Please cite this article in press as: Liu, Y. et al., Tsunami hazards along Chinese coast from potential earthquakes in South China Sea, Phys. Earth Planet. Interiors (2007), doi:10.1016/j.pepi.2007.02.012

bility $P_{e,i}$ of an earthquake i is estimated on the basis of the Gutenberg–Richter (GR) relationship (Gutenberg and Richter, 1949), which relates the frequency of earthquakes with a given magnitude range. Second, to arrive at the probability of the forecast of seismic hazard $P_{PFSH,i}$, one needs to multiply the major earthquake probability $P_{e,i}$ by $P_{oc,i}$, the probability of these earthquakes occurring in the oceanic area. Third, $P_{PFSH,i}$ is further reduced by probability $P_{sh,i}$ of the oceanic earthquakes occurred in shallow depth ($\geq$10 km) in all of events. And finally, since the tsunami wave modeling is based on the effect of rupture length being equal to the entire seismic zone, the epicenter decided randomly, the influence of the rupture length as compare to the whole seismic zone will need to be further reduced by a factor $P_{f,i}$. This computation can be expressed by the following Eq. (4) for the joint probability, which, for the first time, has taken all the above four sources into account.

$$P_{PFSH,i} = P_{e,i} P_{oc,i} P_{sh,i} P_{f,i} \quad (1)$$

where i is the sequential number of the forecasted earthquakes.

At this point a few words are needed to explain our rationale based on the law of total probability (e.g. Wilks, 2006) in deducing the joint probability. According to the theory of plate tectonics, large-scale interplated earthquakes occur near the global subduction zone where the potential energy of elastic strains accumulated over tens to hundreds of years is released over a very short period of time. In this work, estimated the probability of the major earthquake with PFSH, we also take into account together the tectonic evolution, the GPS velocity field, and present-day geophysical stress field, which were analyzed above. For predicting possibility of the earthquake occurrence, the most common treatment (Reiter, 1990) assumes that the frequency of seismic events follow the Gutenberg–Richter relationship. As a phenomenological tool based for estimating the probabilistic analysis of seismic hazrad, the GR relationship has been widely applied for decades since its introduction in late forties. This relationship can be written as (Lomnitz, 1974):

$$\log N = a - bM \quad (2)$$

where N is the cumulative total number of earthquake within a certain period of time for a given magnitude rang and M is the magnitude of the earthquake in any linear or intensity scale or the log of seismic moment (Krinitzsky, 1993). The GR relationship also holds when N is the earthquake number for particular regions or specific time intervals. Parameters a and b are empirical constants derived for each region. Determined from the slope of a frequency–magnitude plot, b depends on the relative proportions of small, medium, and large shocks.

The seismic magnitude frequency data can also be well described, as one or more populations, each of which is normally distributed with respect to the magnitude. This holds true for large earthquakes, when it is sorted out by global subduction zone with the general USGS, NEIC catalog (Speidel and Mattson, 1997). For the PFSH method building, we first study the GR relationship along the global subduction zone. We have divided the global subduction boundaries into nine regions (Fig. 4(a)). Here we have also employed NEIC database. The GR relationship computation of each region verifies the log-linear relationship between the magnitude and the number of events in the history (Fig. 4(b)). Furthermore, our prediction of the earthquake occurrence probability $P_{e,i}$ is based on the above approach.

We estimate sequently the probability $P_{e,i}$ of each particular earthquake magnitude, from 6.5 to 8.0, of the South China Sea and the adjacent areas based on the seismic record of the past 30 years in this region. Database is also derived from NEIC. We only consider the contribution from shallow earthquakes ($P_{sh,i}$) (Fig. 5(b)) with a depth less than 10 km. Only large-scale shallow earthquake can produce large vertical displacement of the seabed and trigger the subsequent tsunami. Here we only consider the major earthquakes with magnitudes larger than 6.0. According to the earthquake distribution, focal mechanism solutions and the tectonic structure of these regions, we partition the South China Sea and its adjacent regions into two parts in order to locate the position of the epicenter of earthquakes used for tsunami modeling. Earthquakes in each part all satisfy the local statistical distribution of the GR relationship (Fig. 5(c)). Because we cannot accurately decide the epicenter for tsunami modeling, we must take account that every fault takes a portion of each seismic zone. This probability is expressed as $P_{f,i}$. The fault size or the surface rupture length is linearly related to earthquake magnitude distribution (Wells and Coppersmith, 1994; Bonilla et al., 1984).

4. Numerical modeling potential tsunami sources

To estimate the near-field tsunami potential hazard for the South China Sea, the linear shallow water equation is applied to describe tsunami generation and subsequent wave propagation.

The initial wave of the linear shallow-water wave equation is computed according to Okada's elastic solution (Okada, 1985), which predicts the water level

Please cite this article in press as: Liu, Y. et al., Tsunami hazards along Chinese coast from potential earthquakes in South China Sea, Phys. Earth Planet. Interiors (2007), doi:10.1016/j.pepi.2007.02.012

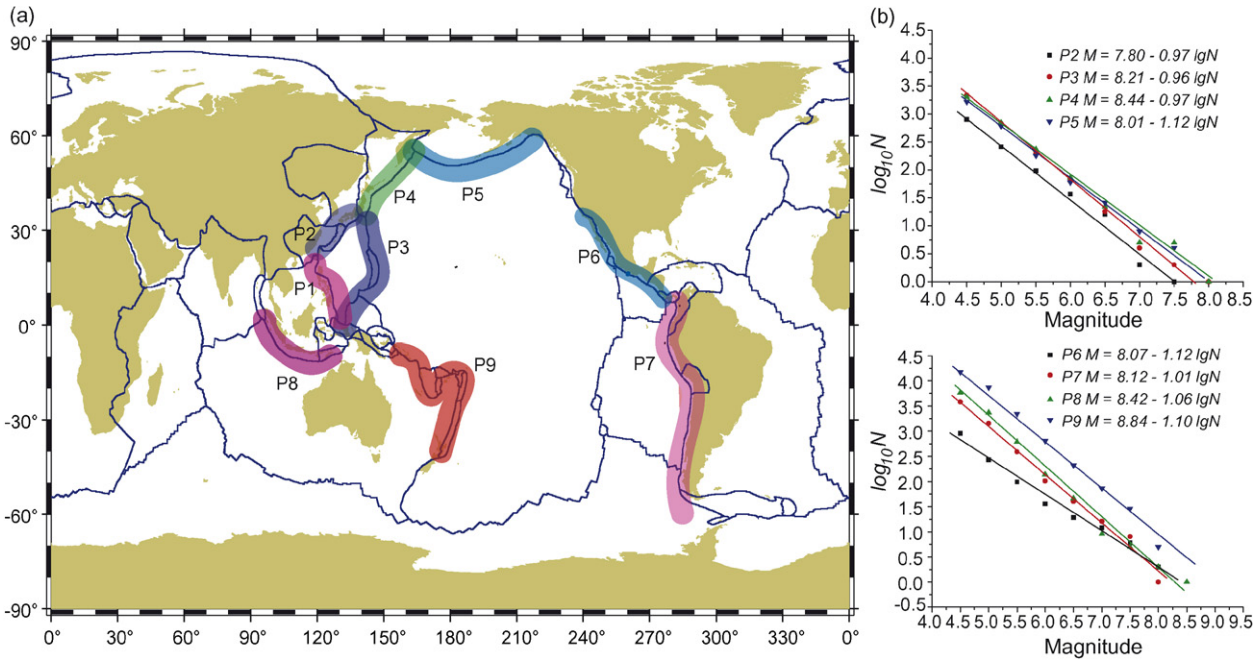

Fig. 4. The global subduction and the GR relationship of global subduction (b) evaluated in this study. This is divided into nine partitions (a). The relation for *P*1, the local study area is separately evaluated in Fig. 5. Boundary subduction data are derived from Bird (2003).

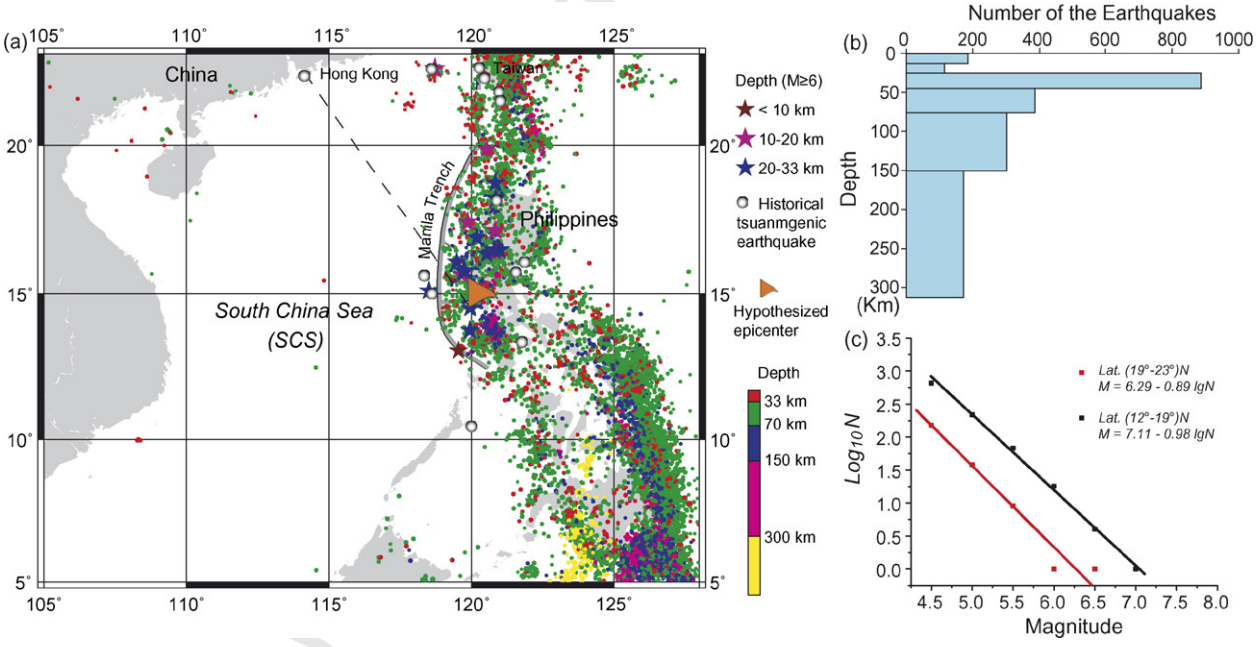

Fig. 5. The earthquakes distribution with the epicenter depths in South China Sea and its adjacent regions (a). Major shallow earthquakes with magnitude over 6.0 are marked with star symbols. Database is derived from NEIC. We divide it into two partitions for deciding the epicenter. The distribution of the number of the earthquakes at different epicenter depth (b). The relationship of local subduction (c). Grey balls represent the historical seismic tsunamis catalog from NGDC/NOAA. The marked hypothetical epicenter is used in Fig. 9. A total of 31 receivers are placed on a straight line from the epicenter to Hong Kong.

Please cite this article in press as: Liu, Y. et al., Tsunami hazards along Chinese coast from potential earthquakes in South China Sea, Phys. Earth Planet. Interiors (2007), doi:10.1016/j.pepi.2007.02.012

changes with numerical integration. A model with a 2D fault embedded in an elastic half-space was adopted to represent major faults of the seismic origin to be used for the tsunami waves induced by an earthquake. The number of earthquakes is computed according to PFSH.

Taken the historical seismic records into account, we divide the computation area into five zones (Fig. 3). As discussed in the previous Section 2, the Manila Trench is the region with the highest possibility for the tsunami occurrence of tsunamogenic earthquakes. We establish four earthquake regions in this area. Since there are also deep faults in the northwestern part of the South China Sea Basin with a history of tsunamogenic earthquakes, one earthquake region is also placed in this area. Within each of the five zones, the earthquakes are sampled with the epicenter randomized according to a modified GR distribution. For the characteristic model, the earthquake magnitudes are defined between the magnitudes of 6.5 and 8.0, with an interval of 0.5.

In the seismic rupture models, source parameters (rupture length L, width W, and the average slip D) are derived from both the theoretical and empirical relationship (Wells and Coppersmith, 1994) which has been widely applied. The fault planes were chosen in accordance with the seismotectonic situation. The fault dips and strikes from the composite fault plane solutions are used as the average dip of the fault segments according to the HCMT catalog. The rupture area of each earthquake does not extend outside individual seismic zone in our modeling.

The average depth of the South China Sea field is from 4 to 5 km. The depth of Manila Trench is around 4.8–4.9 km and reaches the deepest point of 5.4 km. Since the shallow water region is relatively narrow in this region, we employ the linear shallow-water theory in the Cartesian system. Due to the lower latitude of the South China Sea, and the short distance involved, we neglect the Coriolis effect. We have ignored the bottom friction in the computation. The following linear shallow-water equations are applied in our modeling (Goto et al., 1997):

$$\frac{\partial \eta}{\partial t} + \frac{\partial M}{\partial x} + \frac{\partial N}{\partial y} = 0, \qquad \frac{\partial M}{\partial t} + gh\frac{\partial \eta}{\partial x} = 0 \tag{3}$$

where η is sea level displacement, t time, x and y are horizontal coordinates along the zonal and meridional directions, respectively, M and N discharge fluxes in the horizontal plane along x and y coordinates, $h(x,y)$ unperturbed basin depth, and g is the gravity acceleration.

In our numerical simulations, we use the tsunami propagation model Tunami-N1, developed in Tohoku University (Japan) and which is provided through the Tsunami Inundation Modeling Exchange (TIME) program (Goto et al., 1997). The model solves the governing equations by a finite difference technique with the leap-frog scheme (Goto et al., 1997). We use open boundary condition in the model, which permits free outward passage of the wave at the open sea boundaries. The bathymetry of the South China Sea was obtained from the Smith and Sandwell's model of global seafloor topography (Etopo2) with a grid resolution of around 3.8 km. The total number of grid points in the computational domain is 361,201, which is 601 × 601 points. The time step is selected as 1.0 s to satisfy the temporal stability condition. The duration time of wave propagation is 6 h in our simulations.

5. Probabilistic forecast of tsunami hazard

We use computational methods similar to PFSH to develop our probabilistic forecast of the tsunami hazard (PFTH). The probabilistic risk of tsunami is estimated by a combination of large earthquake occurrence probability and the numerical simulation results from tsunami wave propagation:

$$P_{\mathrm{PFTH}}(x, y, h) = \sum_{i=1}^{m} P_{\mathrm{PFSH},i}\{\max(f(x, y), t)\} \tag{4}$$

where P_{PFTH} is the probability of a particular wave height (h) of tsunami in the position x,y along the coast. x,y are the latitude and longitude of the receivers. $P_{\mathrm{PFSH},i}$ is the probability of attaining a maximum wave height from each tsunamogenic earthquake. It is derived from PFSH, Eq. (1). i is the index of the earthquakes. Here m, the number of earthquakes, is 13. $f(x,y)$ is the wave height of tsunami. t is the time of wave propagation. In this work, and the range of t is from 0.0 to 6.0 h. This case provides an method of how the cumulative or joint probability can be calculated for the spatial variability in the probability pattern.

For local tsunamis hazard analysis, we first examine a scenario in which the inter-plate thrust along the Manila subduction zone and the north-western part faults of the South China Sea (Fig. 3). To estimate precisely the probability of tsunami hazards around the South China Sea, 13 seismic tsunami models with magnitudes ranging from 6.5 to 8.0 are computed in five hypothetical epicenters (Fig. 3). Snapshots of a single simulated tsunami wave propagation are shown in Fig. 6. This hypothetical seismic event occurs southwest to the Philippines (14.5°N, 119.2°E), with a magnitude of 7.5. Tsunamis occurring at this location are furthest from the mainland Chinese coast. Due to the relatively long propagation time and very strong wave energy of this tsunami, strong

Please cite this article in press as: Liu, Y. et al., Tsunami hazards along Chinese coast from potential earthquakes in South China Sea, Phys. Earth Planet. Interiors (2007), doi:10.1016/j.pepi.2007.02.012

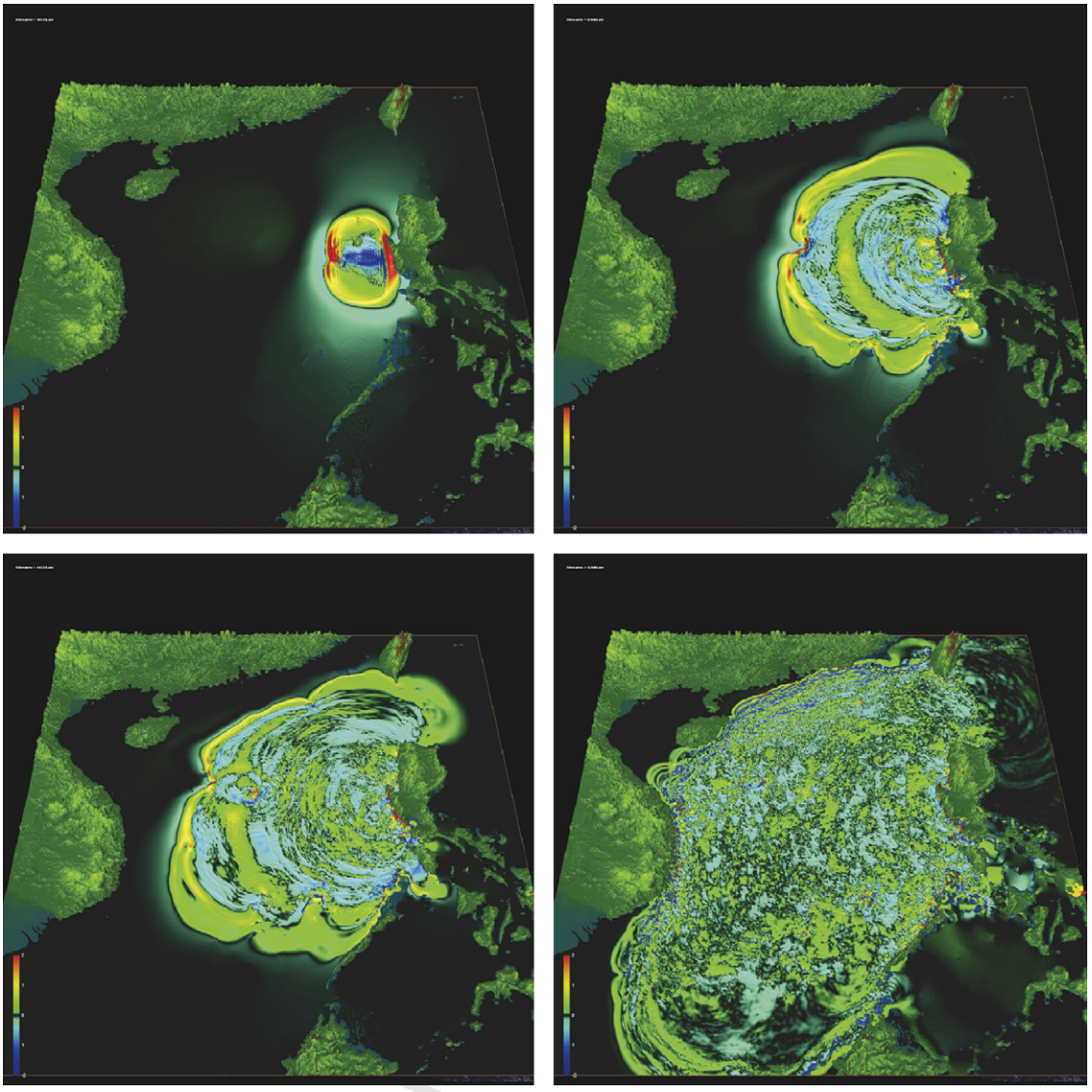

Fig. 6. Visualization of the linear tsunami wave propagation at four different times: 12 min, 72 min, 215 min and 484 min. Two meters represents the maximum height shown.

oscillations and reflection and interference characteristics of tsunami waves can be well observed near islands, such as Xisha, Dongsha and Penghu Islands. Wave diffraction is also obvious among Taiwan island and Philippines, and among the small islands of the south Philippines. In the simulation, tsunami waves are well absorbed along the open boundaries near Taiwan Island. No abnormal computational values have been observed. The wavefronts propagates steadily forward in our computation. Overall, the analysis from various standpoints indicates that the numerical results are stable.

To further validate the wave propagation process, 39 wave receivers at different depth are placed along a straight line between the epicenter and Hong Kong (Fig. 5). The epicenter is at the same place as above earthquake with the magnitude 8.0. Temporal variation of tsunami waves are recorded observed at these points. As shown in Fig. 9, one receiver at deep water region, the depth is 1806.0 m; and another two at shallow water region, the depths are 12.0 m, 75.0 m are illustrated. Waves propagate steadily in deep water region, the effects from reflective waves are minimal. The wave oscillation is dominated by the global maximum value of the wave height. Other local maximum values are much smaller. In the shallow water regions, due to the interference with reflected waves, the magnitudes of all local

Please cite this article in press as: Liu, Y. et al., Tsunami hazards along Chinese coast from potential earthquakes in South China Sea, Phys. Earth Planet. Interiors (2007), doi:10.1016/j.pepi.2007.02.012

maximum wave height values are comparable with the global maximum value.

Altogether 56 coastal receiver points are placed along the mainland coast of the South China Sea, Hainan, and Taiwan Island. For each coastal receiver, the tsunami maximum positive amplitudes are recorded over a sufficiently long amount of time. Our P_{PFTH} computation is based on the maximum wave height of all seismic tsunami together with the occurrence probability of each synthesized tsunami. Two tsunami wave height region of [1.0 m, 2.0 m] (Fig. 8(b)) and heights over 2.0 m (Fig. 8(a)) are considered for our tsunami hazard prediction. Along the south-eastern coast of mainland and Southwestern Taiwan, in Fig. 8(a), we show the distribution for above 2.0 m high tsunami wave hitting. Shown in Fig. 8(b), the same place, together with south-eastern Taiwan, also have a potential chance be beaten with tsunami hazard for 1.0–2.0 m. The computed results of tsunami hazard probability in the next 100 years of major cities along the coast of mainland China are shown in the Table 2. The cities (Fig. 7) of Shantou, Xiamen and Hong Kong are under direct impact from the tsunami earthquakes originated from the central basin of the South China Sea, the southwest and northwest of the Philippines. The tsunami-risk probabilities of these three cities are high, around 10%. Tainan, Kaoxiong and Nawan, three major cities of Taiwan Island are directly affected by the tsunami occurred in the western part of the central basin of the South China Sea and the north Manila Trench. However, the historical seismic records show that the earthquake with a magnitude higher than 7.0 are rare in the oceanic area close to Taiwan, the probability of tsunami wave height higher than 2.0 m in this century (3.44%) in these regions are lower than that in the Hong Kong region (≥10%).

Table 2
The tsunami hazard probabilities of major cities along China Coast in the next 100 years (the cumulative column comes from the sum of the first two columns)

City	Probability in this century		
	Wave height		Cumulative probability (≥1 m (%))
	>2 m (%)	1–2 m (%)	
Shantou	13.34	30.65	43.99
Xiamen	0.00	0.00	0.00
Hong Kong	10.12	17.19	27.31
Macau	10.12	17.19	27.31
Haikou	0.00	0.00	0.00
Sanya	0.00	3.44	3.44
Taitung	0.00	0.00	0.00
Tainan	3.44	17.19	20.63
Kaoxiong	3.44	17.19	20.63
Nanwan	3.44	17.19	20.63

The tsunami hazard probability along the Coast of the South China Sea is plotted in Fig. 8. As shown in this figures, from Shantou to Hong Kong, Macau, the south-

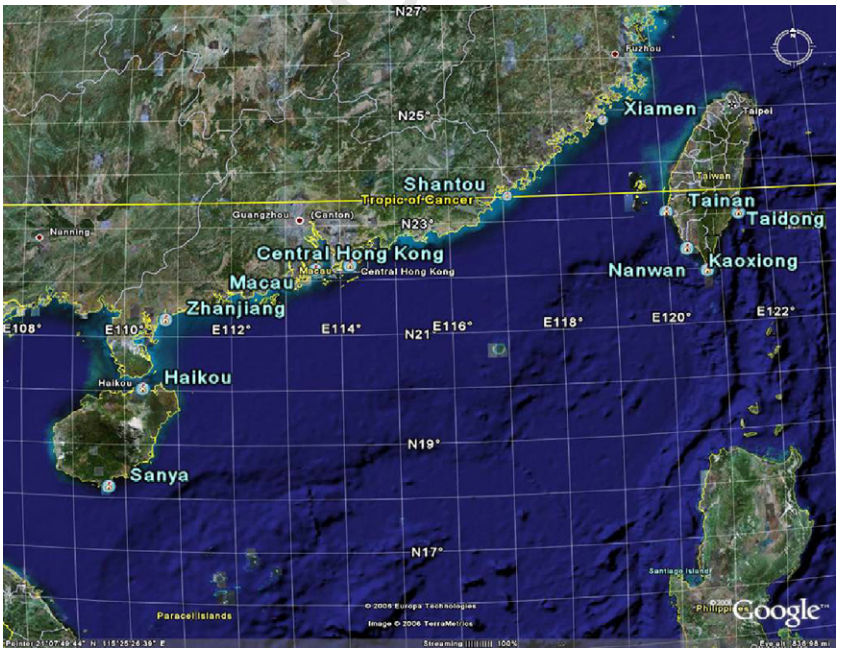

Fig. 7. Major cities along the South China Sea coast.

Please cite this article in press as: Liu, Y. et al., Tsunami hazards along Chinese coast from potential earthquakes in South China Sea, Phys. Earth Planet. Interiors (2007), doi:10.1016/j.pepi.2007.02.012

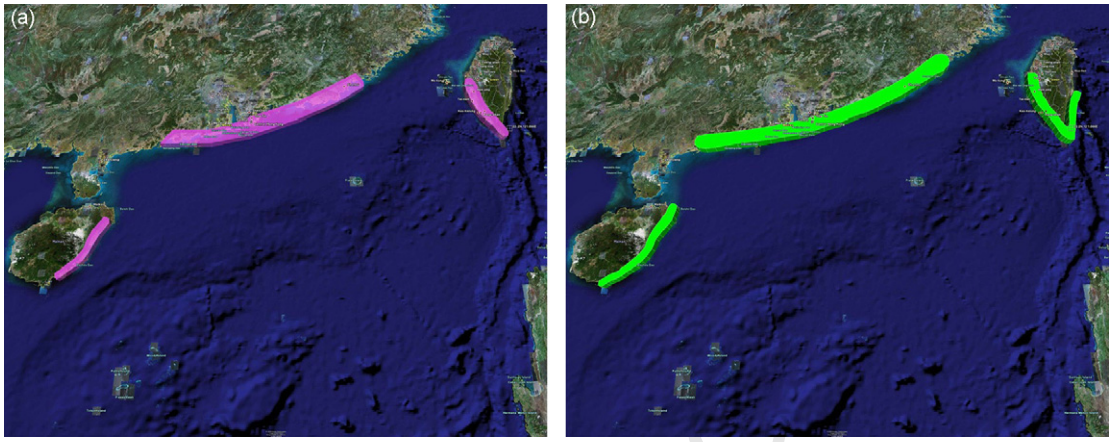

Fig. 8. The spatial distribution of tsunami wave height impinging on the Chinese coast. (a) The case where the wave height is taller than 2.0 m; (b) for the wave height lies between 1.0 and 2.0 m.

west portion of Taiwan island, the east Hainan island are all in harm's way from tsunamis with wave heights more than 2.0 m tall.

6. Discussion and summary

In this section, we discuss first the validity of the linear model. The relationship of our simplified simulation resulting from a single shock and probability of disaster occurrence in complex realistic scenarios is also explained. In addition, effects of specific characteristics of various regions on tsunami hazards are considered.

The South China Sea is an ideal area for conducting simulations of tsunami, waves with a linear model. While the water depth in this area varies from 7000 m to around 10 m, over three-fourth of this area is deeper than 500 m, and the shallow water region is narrow. To further validate the linear model, a simulation based on nonlinear model is conducted in a region in South China Sea. The epicenter selected is near the southwest of Manila Trench with a magnitude of 8.0. Receivers are also placed along the line (Fig. 5) between Hong Kong and the epicenter to validate the wave propagation. In Fig. 9, we compare the wave propagation computed between the linear and nonlinear models. We consider the seabed friction in the nonlinear model. For estimating bottom friction easily, the Manning roughness n replaces the friction with the relationship between f and n (Goto et al., 1997). In our nonlinear model, the value $n = 0.025$ is suitable for the natural channels in good condition which is valid for the South China Sea regions. It has been found in our simulation that there is one critical region between 400 and 500 m depth (Liu et al., 2007). For the deeper seas, both linear and nonlinear models generate similar wave shapes and wave magnitudes. With the ratio of wave height to water depth smaller than 0.01, wave propagation can be modeled by linear theory with reasonable accuracy. Otherwise, the nonlinear model is necessary for shallow depths (see top two panels in Fig. 9). We select four receivers (Fig. 9) at different water depths. At the water depth of 1806 m, the temporal variations of the wave recorded are almost identical between both the linear and nonlinear variations. The maximum wave heights at depth of 12 and 75 m are also identical for both cases. However, differences can be observed for other local maximum values in the sequential wave propagation. Due to the prevalence of deep regions in the South China Sea, we expect the linear model to perform well.

To make sure the results from our linear model are valid, numerical simulations have been conducted with nonlinear model in all 13 tsunami events. With the nonlinear model, the probability is the same for the same tsunami wave height at Hong Kong and Macau, and Kaoxiong, is 10.12%, while a lower probability at Shantou of 10.12% is found with more than 2.0 m to hit within the next 100 years, compares to 13.34% in the linear model. In general, the PFTH for most coastal cities would not change with the usage of nonlinear theory.

Our simulation considers the consequent result from the coseismic generation of the wave by a single shock. Thus a single large wave in the epicentral zone is selected as the initial input for the wave simulation. In reality, the rupture of an earthquake is not simple. The actual generated waves do not come from the wave due to one single shock. During the earthquake occurrence, waves are propagated outwards in the form of wavelets by the continuous rupture dynamics. The constructive combination of the original waves and the following waves of

Please cite this article in press as: Liu, Y. et al., Tsunami hazards along Chinese coast from potential earthquakes in South China Sea, Phys. Earth Planet. Interiors (2007), doi:10.1016/j.pepi.2007.02.012

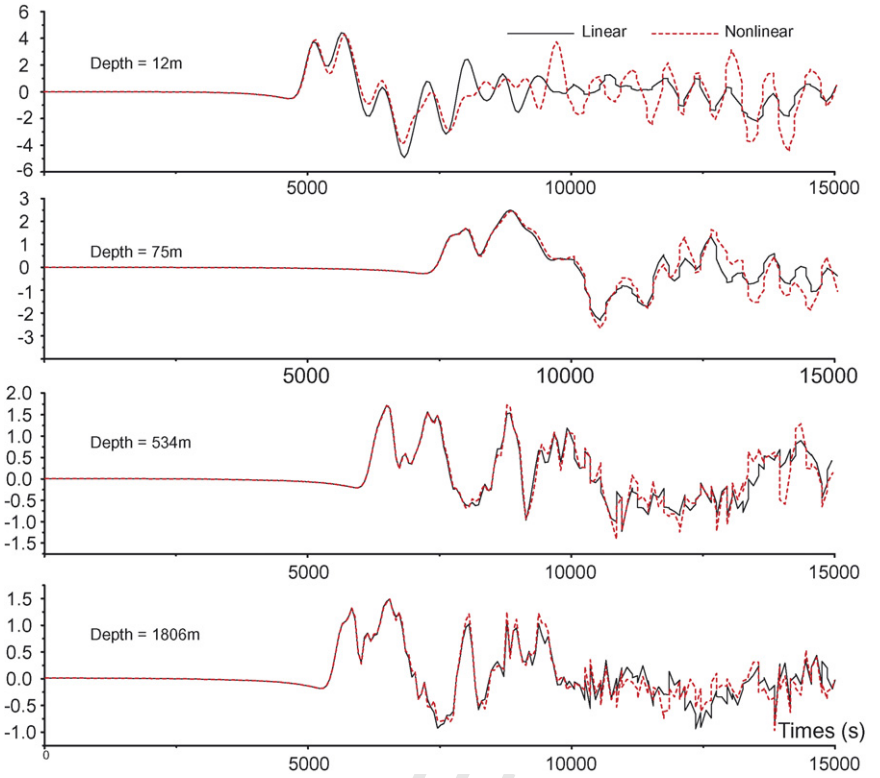

Fig. 9. The temporal variation of the wave height of the linear model at $h = 12$ m, 75 m, 534 m, and 1806 m (Only the results of the first 4 h are plotted).

a tsunami could generate even more dangerous hazard. Based on these facts, our modeling provides an estimate of the lower bound of the hazard possibilities.

The geological and geophysical backgrounds of South China Sea and its adjacent areas are extremely complex. Much effort has been devoted to the research of this region. Literature of historical seismic records of this region is also abundant. Tsunamis occurring at the southwest of Taiwan and Hong Kong have been recorded in the ancient Chinese literature and modern global tsunami catalogues, the largest earthquake occurred at the north part of Manila Trench and the northeast part of the South China Sea has the magnitude around 7.0.

Although the magnitude of this recorded earthquake is only moderately high, considering its proximity to the island of Taiwan, and the coast of Fujian and Guangdong, such a earthquake would very likely cause a tsunami catastrophe. The region between the north part of the Manila Trench near Taiwan is also the boundary between the Eurasia plate and the Philippine Plate with a plate transitional boundary belt. This region is likely to have a very large earthquake in the future. In addition the region is a volcanic belt. If volcano and earthquake occur in concert, a much larger tsunami disaster would develop.

Although the southern part of the Manila Trench is far away from the coast of China, the local historical records of this region have many tsunami earthquakes up to the magnitude of around 8.0. Since the oceanic portion of the South China Sea is mostly deep, tsunamic wave generated in the Manila Trench region can reach the coast of China with little loss in energy. The wave energy can then be released in the shallow water region, and can impose a tremendous tsunami hazard to the coastal regions.

7. Conclusion

The recent pair of earthquakes off the coast of southern Taiwan has forced us to consider more deeply about the possibilities of tsunamis impinging on the coastline of the South China Sea and to develop a simplified probabilistic forecast model. The USGS working group (Kirby et al., 2005) have already met and characterized the western Pacific subduction zones relevant to potential tsunami sources. They also recognized the potential danger coming from the Manila Trench, i.e., the Luzon trough, facing the South China Sea, which might have been overlooked in the past. More systematic work is

Please cite this article in press as: Liu, Y. et al., Tsunami hazards along Chinese coast from potential earthquakes in South China Sea, Phys. Earth Planet. Interiors (2007), doi:10.1016/j.pepi.2007.02.012

needed in collecting more historical records, seismological and geodetic data, which will allow a better assessment of the stress build-up in this region and the potential occurrence of a large-scale earthquake exceeding magnitude 8.5. We have carried out a comparison of linear and nonlinear predictions of tsunami wave propagation across the South China Sea. Our analysis shows that we can apply linear theory to a adequate accuracy in this region. This finding would allow a much quicker earlier warning to be issued, since the linear calculations can be done on laptop computers in nearly real time. The same usage of linear theory for the probabilistic forecast may not hold for the Yellow Sea region because of its much shallower depth and we are carrying out work with the nonlinear model. Finally, this work will hopefully alert people in Hong Kong, Macau and other coastal cities around the South China Sea to the potential hazard of tsunamis coming from the Manila Trench. The probability for this devastating scenario of a 2.0 m wave hitting Hong Kong or Macau is around 10% for this century. This probability estimate may increase with a recent rise in the earthquake activities, which started with the 1999 Chi-Chi earthquake, because the Taiwan region has a earthquake cycle time of around 80–100 years (Lee et al., 2003).

Acknowledgments

We would like to thank Professor Fumihiko Imamura for his providing computational codes TUNAMI_N1 and TUNAMI_N2, and his kind guidance on tsunami numerical method. We would also like to thank Motoyuki Kido and Xiaoru Yuan for their help in preparing this paper. We also thank Willie Lee for discussions. This research is supported by National Natural Science Foundation of China (NSFC-40574021, 40676039) and the EAR program of the U.S. National Science Foundation.

References

Becker, M., Reinhart, E., Nordin, S.B., Angermann, D., Michel, G., Reigber, C., 2000. Improving the velocity field in South and South-East Asia: the third round of GEODYSSEA. Earth Planets Space 52, 721–726.

Bird, P., 2003. An updated digital model of plate boundaries. Geochem. Geophys. Geosyst. 4 (3).

Bonilla, M., Mark, R., Lienkaemper, J., 1984. Statistical relations among earthquake magnitude, surface rupture, and surface fault displacement. Bull. Seismol. Soc. Am. 69, 2003–2024.

Geist, E.L., Parsons, T., 2006. Probabilistic analysis of tsunami hazards. Natural Hazards 37, 277–314.

Goto, C., Ogawa, Y., Shuto, N., Imamura, N. 1997. Numerical method of tsunami simulation with the leap-frog scheme. IUGG/IOC Time Project. IOC Manual, UNESCO 35.

Gutenberg, B., Richter, C.F., 1949. Seismicity of the Earth and Associated Phenomena. Princeton University Press, Princeton.

Kirby, S., Geist, E., Lee, W.H., Scholl, D., Blakely, R., October 2005. Tsunami source characterization for western Pacific subduction zones: a perliminary report. Report, USGS Tsunami Subduction Source Working Group.

Krinitzsky, E., 1993. Earthquake probability in engineering—Part 2: Earthquake recurrence and limitations of Gutenberg Richter *b* values for the engineering of critical structures. Eng. Geol. 36, 1–52.

Lee, W., Kanamori, H., Jenning, P., Kisslinger, C., 2003. International Handbook of Earthquake and Engineering Seismology, Part A. Elsevier, Amsteram.

Liu, Y., Shi, Y., Liu, H., Wang, S.M., Yuen, D.A., May, L.X.H., 2007. Can tsunami waves in the South China Sea be modeled with linear theory? In: Submitted to The International Conference on Computational Science (ICCS), Beijing.

Liu, Z., Yang, S., Chen, S., Liu, Y., et al., 1988. South China Sea Geology Tectonic and Continental Margin Extension. Science Press, Beijing (in Chinese).

Lomnitz, C., 1974. Global Tectonics and Earthquake Risk. Elsevier.

Michel, G.W., Becker, M., Reigber, C., Tibi, R., Yu, Y.Q., Zhu, S.Y., 2001. Regional GPS data confirm high strain accumulation prior to 2000 June 4 Mw = 7.8 earthquake at south east Sumatra. Geophys. J. Int. 146, 71–582.

Okada, Y., 1985. Surface deformation due to shear and tensile faults in a half-space. Bull. Seism. Soc. Am. 75, 1135–1154.

Reiter, L., 1990. Earthquake Hazard Analysis: Issues and Insights. Columbia University Press, New York.

Simons, W.J.F., Ambrosius, B.A.C., Nomen, R., 1999. Plate motions in South-East Asia: results of the GEODYSSEA project. Geophys. Res. Lett. 26, 2081–2084.

Speidel, D.H., Mattson, P.H., 1997. Problems for probabilistic seismic hazard analysis. Natural Hazards 16, 165–179.

Wang, F., Zhang, Z.-Q., 2005. Earthquake tsunami record in Chinese ancient books. Chin. Earthquakes 21 (3), p. 09.

Wells, D., Coppersmith, K., 1994. New empirical relationships among magnitude, rupture length, rupture area, and surface displacement. Bull. Seismol. Soc. Am. 84, 974–1002.

Wilks, D.S., 2006. Statistical Methods in the Atmostheric Sciences, second ed. Academic Press.

Wilson, P., Rais, J., Reigber, C., et al., 1998. The GEODYSSEA project: an investigation of the geology and geodynamics of South and South-East Asia. EOS Trans. Am. Geophys. Union 79, 548–549.

Zang, S., Ning, J., 2002. Interaction between Philippine Sea Plate (PH) and Eurasia (EU) Plate and its influence on the movment eastern Asia. Chin. J. Geophys. 45 (01).

Please cite this article in press as: Liu, Y. et al., Tsunami hazards along Chinese coast from potential earthquakes in South China Sea, Phys. Earth Planet. Interiors (2007), doi:10.1016/j.pepi.2007.02.012